Current Opinion in Solid State and Materials Science 20 (2016) 225–230

Contents lists available at ScienceDirect

Current Opinion in Solid State and Materials Science

journal homepage: www.elsevier.com/locate/cossms

Layering transitions at grain boundaries

J.M. Rickman [a,*], J. Luo [b]

[a] Department of Materials Science and Engineering and Center for Advanced Materials and Nanotechnology, Lehigh University, Bethlehem, PA 18015, United States
[b] Department of NanoEngineering: Program of Materials Science and Engineering, University of California, San Diego, La Jolla, CA 92093, United States

ARTICLE INFO

Article history:
Received 28 October 2015
Revised 19 April 2016
Accepted 24 April 2016
Available online 4 May 2016

Keywords:
Phase transition
Modeling and simulation

ABSTRACT

We review various simplified models that have been advanced to describe layering (complexion) transitions at grain boundaries in multicomponent solids. In particular, we first outline lattice-gas, off-lattice atomistic and thermodynamic models that have been employed to investigate phase-like behavior at segregated grain boundaries. The results of these investigations are summarized in the form of complexion diagrams in different thermodynamic planes, and we highlight important features of these diagrams, such as complexion transition lines and critical points. Finally, we describe current issues and provide a future outlook.

1. Introduction

In recent years there has been growing recognition of the importance of the role of structural and chemical transitions associated grain boundaries [1,2,4,5] in determining material properties. More specifically, observations of interface-stabilized "phases", known as complexions [6–8], have prompted investigations that have connected complexion transitions to changes in observed properties [9], including grain-boundary (GB) mobility and sintering behavior [10,11]. These investigations suggest that the ability to control complexion transitions may enable the tailoring of material properties via interfacial engineering. Given this intriguing possibility, it is necessary to understand the thermodynamics of such transitions in greater detail.

There are several approaches to modeling complexion transitions that underline the competing factors that dictate interfacial structure and chemistry. For example, Rickman et al. [12] generalized the lattice-gas model of surface adsorption of de Oliveira and Griffiths [13] to examine layering transitions at both low-and high-angle grain boundaries. This study highlighted the existence of complexion equilibria and associated transitions, as first observed in a regular-solution model by Wynblatt and Chatain [14,15]. In addition, Luo and coworkers employed a phenomenological, thermodynamic model [16–18] to identify GB complexions and developed associated diagrams that summarize regimes of complexion stability. This sharp-interface approach has been used to study complexions in multicomponent systems. We also note that Tang et al. [2] employed a phase-field model to examine complexion transitions and their relative stability while Mishin et al. [3] used a similar model to study grain-boundary premelting in alloys. Finally, Frolov et al. [19] used molecular dynamics simulation of Ag diffusion in bicrystalline Cu to study structural phase transformations at grain boundaries.

In this article, we compare and contrast various simplified models that have been advanced to describe complexion transitions at grain boundaries in multicomponent solids. Our aim is to demonstrate that these models capture much of the essential physics associated with such transitions. After outlining several complexion models and summarizing a few relevant results, we briefly describe the diagrams that highlight regimes of stability and examine how these regimes may be altered as a function of, for example, temperature and stress. Finally, we address some of the outstanding issues in characterizing complexion transitions and in assessing their impact on material properties.

2. Models and methodology

Several complementary models have been proposed to describe the structure and chemistry associated with layering transitions at grain boundaries. We begin with a review of a binary, lattice-gas model in which the elastic interactions between atoms and a boundary are captured using results from the micromechanics of defects [12]. This approach is then extended to an off-lattice, atomistic model that embodies changes in boundary structure and vibrational modes that attend segregation [20]. A thermodynamic model that has been used to determine the stability of premelting-like, intergranular films is then discussed and compared with the other approaches for complexion modeling [16–18].

* Corresponding author.
E-mail address: jmr6@lehigh.edu (J.M. Rickman).

http://dx.doi.org/10.1016/j.cossms.2016.04.003
1359-0286/

2.1. Lattice-gas model

In this first approach, a grain boundary in a binary alloy is modeled using a modified lattice-gas Hamiltonian that reflects both the chemical and elastic interactions inherent in this system. For this purpose, our starting point is a Hamiltonian developed to study surface gas adsorption [13]. This modified, Ising-like Hamiltonian is given by

$$H = -J \sum_{\langle ijk;\, i'j'k' \rangle} n_{ijk} n_{i'j'k'} + \sum_{ijk} V_{ijk} n_{ijk}, \tag{1}$$

where J is an energy parameter, V_{ijk} is an external field, the angle brackets denote a nearest-neighbor summation and n_{ijk} is an occupancy variable equal to zero (one) if a given site is occupied by an A (B) atom. In a regular-solution model, J can be related to the interaction energies $\epsilon_{\alpha\beta}$ between atoms of type α and β. One finds that $J = (\epsilon_{AA} + \epsilon_{BB} - 2\epsilon_{AB})$.

We next extend this model to describe grain-boundary segregation in a bicrystal and associated complexion transitions [12]. In particular, we construct a mean-field grand potential, $\Omega(T, \Delta\mu)$, for a system in contact with a thermal reservoir having a temperature T and with a difference in chemical potential $\Delta\mu$ that reflects the aforementioned lattice-gas energetics. For simplicity, it is assumed that the configurational entropy is given by the ideal entropy of mixing. In this formulation V_{jk} embodies the elastic interactions between the lattice-gas atoms and the grain boundary. The equilibrium state of this system can then be determined by minimizing Ω with respect to the site-occupancy variables.

For the purposes of illustration, two limiting cases for V_{jk} are considered, namely those corresponding to generic low- and high-angle boundaries. In the former case, a low-angle tilt boundary is modeled as an array of edge dislocations [21,22] while, in the latter case, the boundary is regarded as an isotropic slab inhomogeneity that differs elastically from the surrounding medium [23]. In each case the atoms are modeled as spherical centers of dilatation in an (infinite) elastically isotropic medium. For simplicity, symmetric boundaries are employed here, and so only even numbers of segregated layers can be observed. In Section 3, we present complexion diagrams obtained from this analysis that illustrate coexistence between different interfacial states.

2.2. Binary Lennard-Jones system in the semi-grand canonical ensemble

Consider next a binary, atomistic model comprising lattice (A) atoms and impurity (B) atoms that incorporates off-lattice atomic motion and elastic interactions and permits one to vary the relevant intensive parameters, such as the temperature (T), the stress and the difference in chemical potential ($\Delta\mu$) [20]. For simplicity, a modified Lennard-Jones potential [24] having parameters ϵ_{ij} and σ_{ij} (where the subscripts denote atom type), with Lorentz-Berthelot rules [25] used to describe A-B interactions, is employed to capture the energetics of this system. As is customary, energy and length scales are reported in units of ϵ_{AA} and σ_{AA}, respectively. For a periodic simulation cell containing a grain boundary and a choice of interaction parameters, the system is equilibrated for a given T, stress component p_{zz} (where the z-direction in normal to the GB plane) and $\Delta\mu$ in the semi-grand canonical ensemble [26,27].

To study complexion transitions, it is useful to determine the ensemble-average interfacial excess $\Gamma = N_B/N_B^0$ at each boundary, where N_B is the number of B atoms within 3 lattice parameters of a grain boundary and N_B^0 is the maximum number of B atoms in the GB region, as a function of the intensive variables. The calculation of Γ enables the construction of a complexion diagram that highlights complexion coexistence. In practice, this construction is accomplished by recording the fraction of simulation time associated with each value of Γ. From this information, one can then compile a histogram that reflects the associated probability distribution of Γ. This histogram is used, in turn, to plot the associated complexion miscibility gap and, in addition, to obtain the interfacial free energy of coexisting complexions. Some examples of this methodology are discussed in Section 3 below.

2.3. Thermodynamic model

At longer length scales, one can formulate a thermodynamic model of complexion equilibria in alloys by extending existing, sharp-interface models of premelting in single-component systems [28]. In this formulation, the excess GB energy of a (subsolidus) liquidlike intergranular film in an A-B alloy, relative the corresponding bulk phases, can be written as [18,29]

$$\sigma^x(h) = 2\gamma_{cl} + \Delta G^{(vol)}_{amorph} h + \sigma_{interfacial}(h), \tag{2}$$

where h is the effective interfacial width (commonly known as the film thickness), γ_{cl} is the energy of the crystal-liquid interface and $G^{(vol)}_{amorph}$ is the free-energy cost for forming an undercooled liquid [17]. The interfacial potential, $\sigma_{interfacial}(h)$, includes the effects of all interfacial interactions [18,29,30]. A stable subsolidus, liquidlike interfacial complexion may exist with a maximum interfacial width of

$$h < -\frac{\Delta\gamma}{G^{(vol)}_{amorph}} f(h), \tag{3}$$

where $\Delta\gamma = 2\gamma_{cl} - \sigma^x(h=0)$ and the dimensionless interface coefficient, $f(h)$, is defined by

$$\sigma_{interfacial}(h) = -\Delta\gamma(1 - f(h)), \tag{4}$$

with the boundary conditions $f(h=0) = 0$ and $f(h=+\infty) = 1$. From these considerations, it is convenient to define a parameter, λ, that scales the actual interface width as [31]

$$\lambda = -\frac{\Delta\gamma}{G^{(vol)}_{amorph}}. \tag{5}$$

The values of λ can be obtained for specific systems by estimating the relevant interfacial energies using statistical models and by employing bulk phase diagram (e.g., CALPHAD) data and tools. Computed λ values can then be plotted on bulk phase diagrams to construct "GB λ-diagrams", as in several previous studies [11,17,18,29,32]. We note that these diagrams are not rigorous GB complexion diagrams; however, they have been proven useful for forecasting trends in high-temperature GB disordering, activated sintering, Coble creep and other GB-controlled phenomena.

Eq. (2) can also be rewritten in dimensionless form as

$$\frac{\sigma^x(h) - \sigma^x(0)}{-\Delta\gamma} = -f(h) + \frac{h}{\lambda}. \tag{6}$$

The minimization of Eq. (6) with respect to h yields an equilibrium interfacial width, h_{eq}. If the interface coefficient decays exponentially with a characteristic length ξ (i.e., if $f(h) = 1 - \exp(-h/\xi)$) for metals having one dominant short-range interaction, a non-intrinsic GB complexion starts to develop ($h_{eq} > 0$) when $\lambda > \xi$, with an equilibrium interfacial width $h_{eq} = \xi \ln(\lambda/\xi)$. However, the interface coefficient for most real materials can be much more complex and difficult to quantify. More specifically, oscillatory interface coefficients (resulting from discrete atomic sizes) can produce layering transitions. Some examples will be presented in the next section.

3. Complexion diagrams

Complexion coexistence can be summarized in the form of diagrams that highlight regions of complexion stability. In the case of a binary alloy, it is useful to determine, for example, the dependence of the interfacial excess, Γ, on $\Delta\mu$ and thereby identify which complexions are stable at a given temperature, T. For convenience, we define τ, the ratio of T to the critical temperature for the bulk alloy in the mean-field approximation. For the aforementioned lattice-gas model, Fig. 1a shows Γ as a function of the normalized chemical potential, $\Delta\mu/J$ for a prototypical high-angle boundary. For the three temperature ratios shown here, it is evident that the system undergoes a series of first-order layering transitions. This information may be replotted in the form of a complexion diagram in the Γ-τ plane, as shown in Fig. 1b. For the various complexion states there exists a series of miscibility gaps that summarize regimes of complexion coexistence, with each gap terminating in a critical point.

Consider next the binary Lennard-Jones system simulated in the semi-grand canonical ensemble, as described above. In particular, we examine the case of oversized B atoms having $\sigma_{BB} = 1.1$ and $\epsilon_{BB} = 1.1$ in a system with $T = 0.1$ subject to an applied stress $p_{zz} = 3.0$. Fig. 2a shows Γ as a function of the normalized chemical potential, $\Delta\mu/\epsilon_{AA}$ for a Σ 5 (100) twist grain boundary. As in the case of the lattice-gas model (see Fig. 1), one observes a series of layering transitions as a function of $\Delta\mu$, with narrower regions of complexion stability associated with larger values of the chemical potential difference, $\Delta\mu$. Furthermore, simulations at different values of p_{zz} indicate that the locations of complexion transitions can be altered by the imposition of different applied stresses. In Fig. 2b the corresponding miscibility gap for the equilibrium between a bare grain boundary and a single-layer complexion in shown in the Γ-T plane. For this case, a somewhat larger atomic misfit

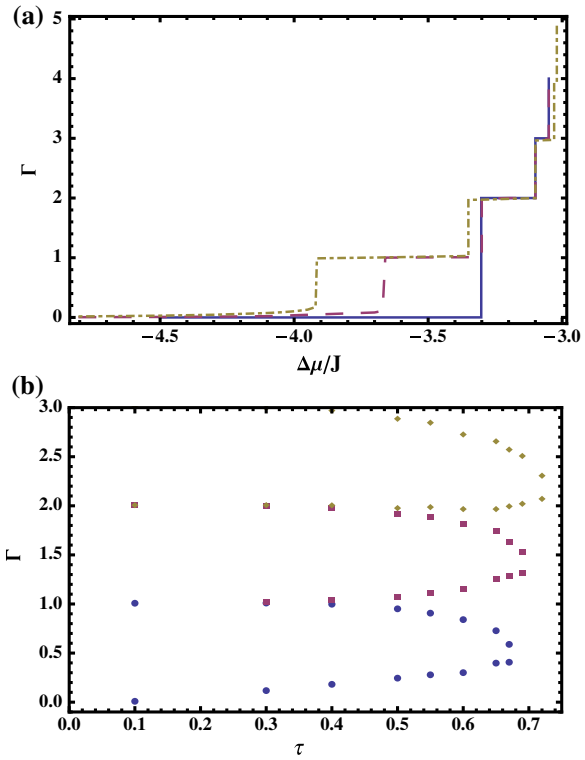

Fig. 1. (a) The excess fraction, Γ, as a function of the normalized chemical potential difference, $\Delta\mu/J$, for temperature ratios $\tau = 0.1$ (solid line), 0.3 (dashed line) and 0.4 (dot-dashed line). (b) The excess fraction, Γ, versus the reduced temperature, τ, for different complexion states. Note the series of miscibility gaps that highlight complexion coexistence. Re-plotted after [12], with permission from Elsevier.

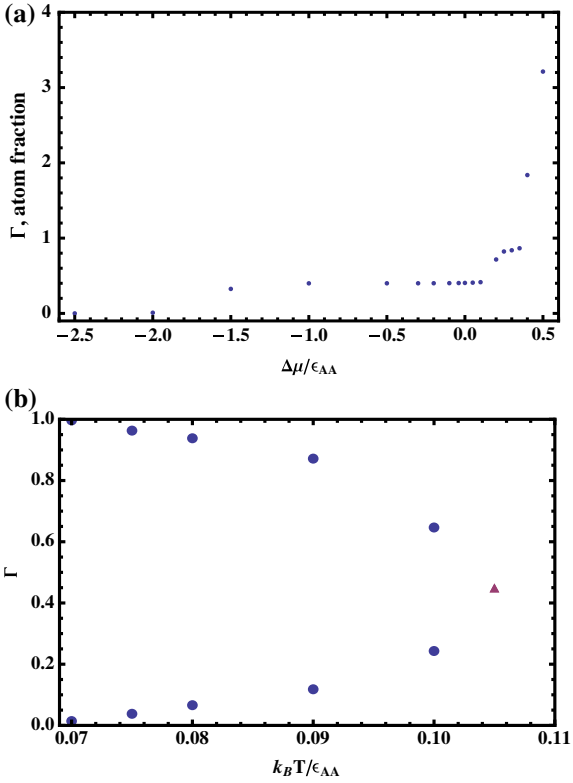

Fig. 2. (a) The excess fraction, Γ, as a function of the normalized chemical potential, $\Delta\mu/\epsilon_{AA}$, for a Σ 5 (100) twist grain boundary for an applied stress $p_{zz} = 3.0$. (b) The excess fraction, Γ, as a function of normalized temperature. The miscibility gap highlighting coexistence between a bare boundary and a single-layer complexion is shown here. For this case, $\sigma_{BB} = 1.13$ and $\epsilon_{BB} = 3.0$ in a system for $p_{zz} = 0.1$. These results come from an atomistic simulation of a binary alloy in the semi-grand canonical ensemble, and are qualitatively similar to those obtained in Fig. 1.

$\sigma_{BB} = 1.13$ and a large interaction energy $\epsilon_{BB} = 3.0$ in a system for $p_{zz} = 0.1$ are employed. This result is qualitatively similar to one of the miscibility gaps obtained for the lattice-gas model (see Fig. 1b).

The aforementioned Wynblatt-Chatain model can also be used to construct complexion diagrams [14]. Fig. 3 displays two equivalent GB complexion diagrams, plotted in both the $\Delta\mu$-T and X-T planes, where X denotes the alloy composition. Wynblatt and Chatain [15] already demonstrated that their model can produce a single prewetting transition. Using a variant of their model, we obtained Fig. 3 using a simplified regular-solution type model of a binary alloy representing an average, large-angle, general twist GB in Ag-doped Ni. Thus, the Wynblatt-Chatain model can also produce multiple layering transitions for a strongly segregating system, similar to those predicted by the model of Rickman et al. [12]. These figures show that at constant temperatures layering transitions produce a series of discrete GB complexions, such as intrinsic (nominally clean) GBs, bilayers, and high-order complexions (4-layers and beyond), with increasing bulk composition (Fig. 3b) or chemical potential (Fig. 3a). These transitions are similar to those predicted by the lattice-gas model discussed above. With increasing temperature, the first-order transition lines may terminate at critical points, beyond which the complexion transitions becomes continuous. We note that this model only produces even numbers of adsorbate layers, due to a mirror symmetry in the twist GBs used in the model.

The lattice models considered here do not permit any interfacial disordering, which may occur at high temperatures near the bulk solidus line. Thus, an alternative approach to complexion modeling regards liquid-like GB complexions as thin layers of a confined

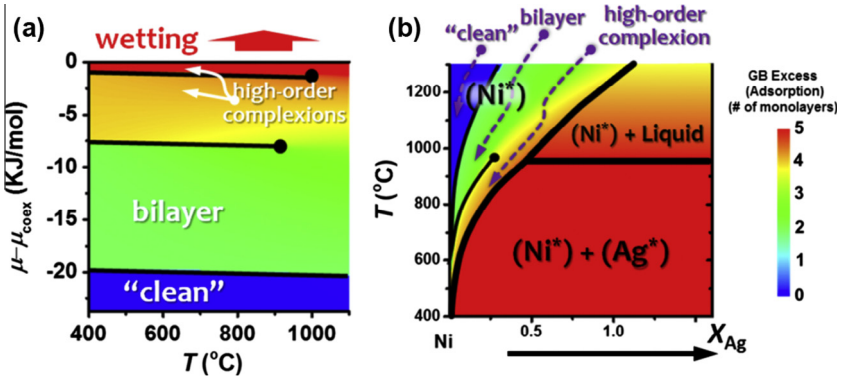

Fig. 3. Computed GB complexion diagrams for a regular-solution type binary alloy with parameters chosen to represent an average, large-angle, general, twist GB in Ag-doped Ni, using the Wynblatt-Chatain model [14]. The equivalent complexion diagrams are plotted in (a) the $\Delta\mu$-T and (b) the X-T planes. The superscripts in Ag* and Ni* are used to indicate that these phases are Ag-like and Ni-like, respectively, and that they may differ somewhat from the real Ag-doped Ni alloy due to simplifications adopted in the model. This is unpublished work, courtesy of Naixie Zhou.

liquid, following the phenomenological thermodynamic model described above. In this approach, layering transitions are produced using structural oscillatory potentials; for a confined hard-sphere liquid with particle diameter δ, colloidal theory indicates that such a potential should have a period of δ with an oscillatory amplitude that decays exponentially [33]. This approach is quite useful in describing observed Dillon-Harmer complexion states (see Fig. 4a).

An example of an exponentially-decaying oscillatory potential, superposed on another exponentially-decaying potential (namely $1-\exp(-h/\xi)$) having a longer characteristic length ξ, is shown in Fig. 4b in the form of a normalized excess GB energy, as expressed by Eq. (6). With increasing undercooling (decreasing λ), a series of GB complexions, corresponding to the minima in the curves, having discrete interfacial widths of h_{eq}/δ can be produced. This series of complexions is similar to the six

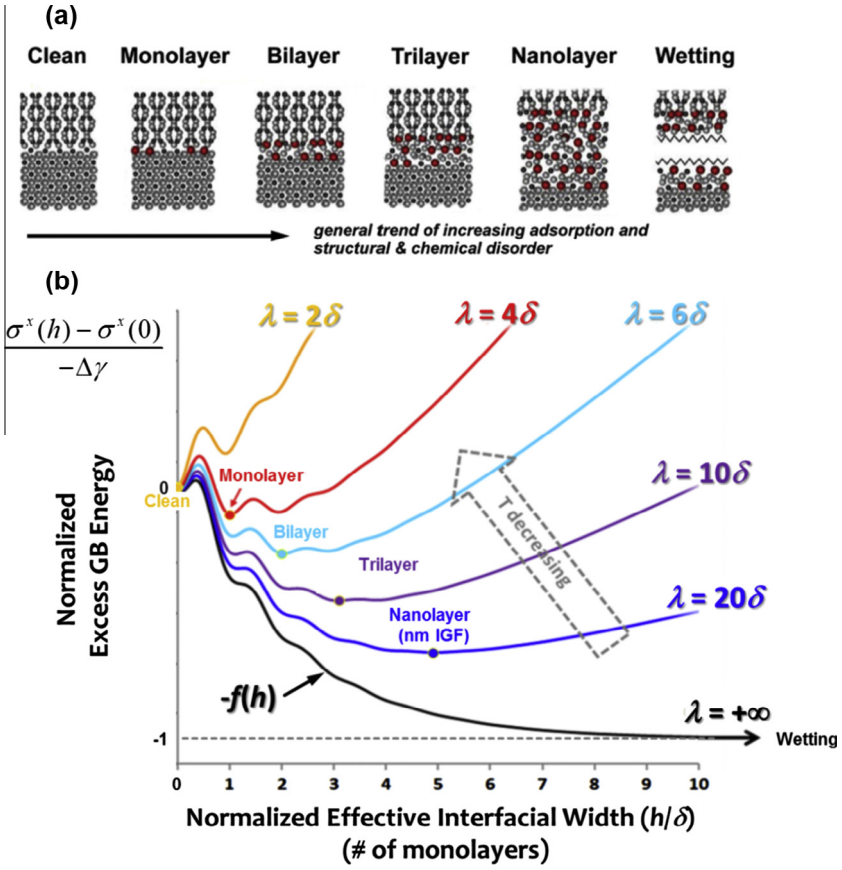

Fig. 4. (a) Schematic illustration of Dillon-Harmer complexions. (b) Schematic plots of normalized excess GB energy vs. normalized interfacial width h/δ, where δ is an atomic distance, indicating the formation of a series of distinct Dillon-Harmer complexions at different undercooling temperatures (represented by λ values). An exponentially-decaying oscillatory interfacial potential is used to represent an undercooled hard-sphere liquid. The normalized excess GB energy is identical to $f(h)$ for the case $\lambda = +\infty$. Panel (a) is reprinted after [4,34] and Panel (b) is replotted after [50], with permissions from Elsevier.

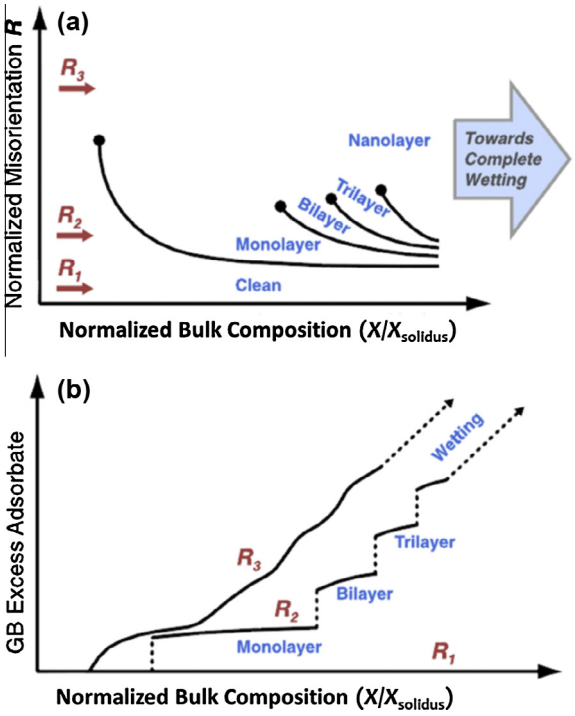

Fig. 5. (a) A computed GB complexion diagram and (b) the corresponding GB excess vs. normalized bulk composition curves for the three selected GBs labeled in (a). Re-plotted after [16], with permission from AIP.

Dillon-Harmer complexions (Fig. 4a) that are observed in both ceramics [4] and metals [8,34].

The sharp-interface model described in Section 2 can be combined with lattice and diffuse-interface models to construct GB complexion diagrams for binary alloys with well-defined layering transitions and critical points [16], as shown in Fig. 5. It should be noted that the effective interfacial width increases with increasing bulk composition continuously above the critical (roughening) points; moreover, layering occurs below the roughening points, leading to stepwise increases in the interfacial width and producing a series of discrete Dillon-Harmer complexions (Fig. 4a). Although one can formulate a more complex description of this phenomenon [16], these layering transitions originate from the same structural oscillatory potential discussed above. It is worth noting that analogous layering transitions have been observed and modeled for surface multilayer gas adsorption on non-reacting, attractive substrates [35].

4. Discussion and conclusions

We have reviewed three simplified models that describe layering (i.e., complexion) transitions at grain boundaries in multicomponent solids. These models predict the occurrence of multiple layering transitions, with each transition having an associated GB critical point. They are useful for describing complexion equilibria and permit the construction of complexion diagrams that summarize regions of stability. It has been demonstrated that complexion transitions are first-order in character and that their locations in parameter space may be altered, for example, by an applied stress.

There are several outstanding issues as to the nature of these transitions and their impact on observed properties. First, one would expect that transition temperatures, etc., will depend on the macroscopic degrees of freedom associated with the boundary, but a systematic study of such dependencies is still lacking. Moreover, while the nature of the transition is evidently first order, and therefore occurs via nucleation and growth, the mechanism of the transition has not been elucidated in any detail [34]. It is also of interest to examine complexion states in systems with many alloying elements, such as high-entropy alloys, where the interactions of multiple segregating elements may produce new interfacial phenomena.

With regard to properties, it is expected that a GB segregant will influence phonon and electron scattering as well as mass diffusion at internal interfaces. For example, in recent work by Goel et al. [36] it was shown that the Kapitza resistance in SiC is dictated, at least in part, by the presence of oversized dopant atoms located at grain boundaries, and therefore by phonon scattering from these segregants. It is also therefore plausible that electrical conductivity will correlate with complexion states in metals owing to differences in electron scattering at segregated boundaries. For functional ceramics, the formation of impurity-based complexions is believed to have a strong impact on electrical [37], thermal [38,39] and ionic [40–42] conductivities, and may affect or even control the critical current of high-Tc superconductors [43], the coercivity of permanent magnets [44] and the rate capabilities and cycling stability of lithium-ion batteries [45–49]. For a more extended discussion of these topics, see the critical review by Luo [30]. Finally, given the structural and chemical changes associated with complexion transitions, it is also likely that reaction pathways for mass diffusion will vary from one complexion state to another. Direct experimental evidence highlighting the impact of complexion transitions on properties is still lacking in many cases, and it is hoped that this paper will motivate such studies.

Acknowledgments

The authors gratefully acknowledge financial support from ONR-MURI under Grant No. N00014-11-1-0678. J.L. also acknowledges partial support from an NSSEFF fellowship (N00014-15-1-0030). We thank Naixie Zhou for the calculations leading to Fig. 3.

References

[1] M. Tang, W.C. Carter, R.M. Cannon, Grain boundary transitions in binary alloys, Phys. Rev. Lett. 97 (2006) 075502.
[2] M. Tang, W.C. Carter, R.M. Cannon, Diffuse interface model for structural transitions of grain boundaries, Phys. Rev. B 73 (2006) 024102.
[3] Y. Mishin, W.J. Boettinger, J.A. Warren, G.B. McFadden, Thermodynamics of grain boundary premelting in alloys. I. Phase-field modeling, Acta Mater. 57 (2009) 3771–3785.
[4] S.J. Dillon, M. Tang, W.C. Carter, M.P. Harmer, Complexion: a new concept for kinetic engineering of materials, Acta Mater. 55 (2007) 6208.
[5] M.P. Harmer, Interfacial kinetic engineering: how far have we come since Kingery's inaugural Sosman address?, J Am. Ceram. Soc. 93 (2010) 301.
[6] M.P. Harmer, The phase behavior of interfaces, Science 332 (2011) 182–183.
[7] M. Baram, D. Chatain, W.D. Kaplan, Nanometer-thick equilibrium films: the interface between thermodynamics and atomistics, Science 332 (2011) 206–209.
[8] J. Luo, H.-K. Cheng, K.M. Asl, C.J. Kiely, M.P. Harmer, The role of a bilayer interfacial phase on liquid–metal embrittlement, Science 333 (2011) 1730–1733.
[9] S.J. Dillon, M.P. Harmer, Relating grain-boundary complexion to grain-boundary kinetics I: calcia-doped alumina, J. Am. Ceram. Soc. 91 (2008) 2304–2313.
[10] J. Luo, Developing interfacial phase diagrams for applications in activated sintering and beyond: current status and future directions, J. Am. Ceram. Soc. 95 (2012) 2358.
[11] J. Luo, X.M. Shi, Grain-boundary disordering in binary alloys, Appl. Phys. Lett. 92 (2008) 101901.
[12] J.M. Rickman, H.M. Chan, M.P. Harmer, J. Luo, Grain-boundary layering transitions in a model bicrystal, Surf. Sci. 618 (2013) 88–93.
[13] M.J. de Oliveira, R.B. Griffiths, Lattice gas model of multiple layer adsorption, Surf. Sci. 71 (1978) 687–694.
[14] P. Wynblatt, D. Chatain, Anisotropy of segregation at grain boundaries and surfaces, Metall. Mater. Trans. 37A (2006) 2595–2620.
[15] P. Wynblatt, D. Chatain, Solid-state wetting transitions at grain boundaries, Mater. Sci. Eng. A495 (2008) 119–125.
[16] J. Luo, Grain boundary complexions: the interplay of premelting, prewetting and multilayer adsorption, Appl. Phys. Lett. 95 (2009) 071911.

[17] X. Shi, J. Luo, Developing grain boundary diagrams as a materials science tool: a case study of nickel-doped molybdenum, Phys. Rev. B 84 (2011) 014105.
[18] N. Zhou, J. Luo, Developing grain boundary diagrams for multicomponent alloys, Acta Mater. 91 (2015) 202–216.
[19] T. Frolov, S.V. Divinski, M. Asta, Y. Mishin, Effect of interface phase transformations on diffusion and segregation in high-angle grain boundaries, Phys. Rev. Lett. 110 (2013) 255502.
[20] J.M. Rickman, M.P. Harmer, H.M. Chan, Grain-boundary layering transitions and phonon engineering, Surf. Sci. 651 (2016) 1–4.
[21] W.T. Read, W. Shockley, Dislocation models of crystal grain boundaries, Phys. Rev. 78 (1950) 275–289.
[22] J.P. Hirth, J. Lothe, Theory of Dislocations, second ed., Krieger Publishing Company, Malabar, Florida, 1992.
[23] P. Deymier, L. Janot, J. Li, L. Dobrzynski, Elastic energy of interaction of a point defect with a grain boundary, Phys. Rev. B 39 (1989) 1512–1517.
[24] J.Q. Broughton, G.H. Gilmer, Molecular dynamics investigation of the crystal-fluid interface. I. Bulk properties, J. Chem. Phys. 79 (1983) 5095.
[25] J.-P. Hansen, I.R. MacDonald, Theory of Simple Liquids: With Applications to Soft Matter, Elsevier, Oxford, 2013.
[26] D. Kofke, E. Glandt, Monte Carlo simulation of multicomponent equilibria in a semigrand-canonical ensemble, Mol. Phys. 64 (1988) 1105–1131.
[27] J.M. Rickman, T.J. Delph, E.B. Webb III, R. Fagan, A numerical coarse-grained description of a binary alloy, J. Chem. Phys. 137 (2012) 054108.
[28] J.G. Dash, A.M. Rempel, J.S. Wettlaufer, The physics of premelted ice and its geophysical consequences, Rev. Mod. Phys. 78 (2006) 695.
[29] J. Luo, Developing interfacial phase diagrams for applications in activated sintering and beyond: current status and future directions, J. Am. Ceram. Soc. 95 (2012) 2358–2371.
[30] J. Luo, Stabilization of nanoscale quasi-liquid interfacial films in inorganic materials: a review and critical assessment, Crit. Rev. Solid State Mater. Sci. 32 (2007) 67–109.
[31] X. Shi, J. Luo, Grain boundary wetting and prewetting in Ni-doped Mo, Appl. Phys. Lett. 94 (2009) 251908.
[32] J. Luo, Liquid-like interface complexion: from activated sintering to grain boundary diagrams, Curr. Opin. Solid State Mater. Sci. 12 (2008) 81–88.
[33] J.N. Israelachvili, Intermolecular and Surface Forces, forth ed., Academic Press, London, 1994.
[34] P.R. Cantwell, M. Tang, S.J. Dillon, J. Luo, G.S. Rohrer, M.P. Harmer, Grain boundary complexions, Acta Mater. 62 (2014) 1–48.
[35] R. Pandit, M. Schick, M. Wortis, Systematics of multilayer adsorption phenomena on attractive substrates, Phys. Rev. B 26 (1982) 5112–5140.
[36] N. Goel, E.B. Webb III, A. Oztekin, J.M. Rickman, S. Neti, Kapitza resistance at segregated boundaries in β-SiC, J. Appl. Phys. 118 (2015) 115101.
[37] Y.-M. Chiang, L.A. Silverman, R.H. French, R.M. Cannon, Thin glass film between ultrafine conductor particles in thick-film resistors, J. Am. Ceram. Soc. 77 (1994) 143–152.
[38] D.L. Callahan, G. Thomas, Impurity distribution in polycrystalline aluminum nitride ceramics, J. Am. Ceram. Soc. 73 (1990) 2167–2170.
[39] H. Nakano, K. Watari, K. Urabe, Grain-boundary phase in AlN ceramics fired under reducing N_2 atmosphere with carbon, J. Eur. Ceram. Soc. 23 (2003) 1761–1768.
[40] G. Harley, R. Yu, L.C. De Jonghe, Proton transport paths in lanthanum phosphate electrolytes, Solid State Ionics 178 (2007) 769–773.
[41] W. Liu, W. Pan, J. Luo, A. Godfrey, G. Ou, H. Wu, W. Zhang, Suppressed phase transition and giant ionic conductivity in $La_2Mo_2O_9$ nanowires, Nat. Commun. 6 (2015) 8354.
[42] J. Luo, Interfacial engineering of solid electrolytes, J. Materiom. 1 (2015) 22–32.
[43] R. Ramesh, S.M. Green, G. Thomas, Microstructure property relations in the Bi (Pb)–Sr–Ca–Cu–O ceramic superconductors, in: A. Narlikar (Ed.), Studies of High Temperature Superconductors: Advances in Research and Applications, Nova Science Publ., Commack, NY, 1990, pp. 363–403.
[44] O. Gutfleisch, M.A. Willard, E. Brück, C.H. Chen, S.G. Sankar, J.P. Liu, Magnetic materials and devices for the 21st century: stronger, lighter, and more energy efficient, Adv. Mater. 23 (2011) 821–842.
[45] B. Kang, G. Ceder, Battery materials for ultrafast charging and discharging, Nature 458 (2009) 190–193.
[46] A. Kayyar, H.J. Qian, J. Luo, Surface adsorption and disordering in $LiFePO_4$ based battery cathodes, Appl. Phys. Lett. 95 (2009) 221905.
[47] K. Sun, S.J. Dillon, A mechanism for the improved rate capability of cathodes by lithium phosphate surficial films, Electrochem. Commun. 13 (2011) 200–202.
[48] J. Huang, J. Luo, A facile and generic method to improve cathode materials for lithium-ion batteries via utilizing nanoscale surface amorphous films of self-regulating thickness, Phys. Chem. Chem. Phys. 16 (2014) 7786–7798.
[49] M. Samiee, J. Luo, A facile nitridation method to improve the rate capability of TiO_2 for lithium-ion batteries, J. Power Sour. 245 (2014) 594–598.
[50] S. Ma, P.R. Cantwell, T.J. Pennycook, N. Zhou, M.P. Oxley, D.N. Leonard, S.J. Pennycook, J. Luo, M.P. Harmer, Grain boundary complexion transitions in WO_3- and CuO-doped TiO_2 bicrystals, Acta Mater. 61 (2013) 1691–1704.